SCIAMACHY Level 2 Version 6 Nitrogen Dioxide Column Validation

Kai-Uwe Eichmann, Mark Weber, and John P. Burrows
Institut für Umweltphysik, Universität Bremen, Bremen, Germany

Document Number	:	scilov15_no2_v11
Version	:	1.1
Date	:	December 12, 2017

Contact	:	Kai-Uwe Eichmann (eichmann@uni-bremen.de) Universität Bremen FB1 P.O. Box 330 440 D-28334 Bremen

Status	:	final draft

Contents

1 Introduction

SCIAMACHY (SCanning Imaging Absorption spectroMeter for Atmospheric CHartographY) (Burrows et al., 1995; Bovensmann et al., 1999) was launched in 2002 and provided nadir, limb, and occultation measurements until the loss of contact with ENVISAT in April 2012.

The ESA project SCILOV-15 (SCIAMACHY long term validation 2015) aims at the lifetime validation and documentation of the quality of various operational data products retrieved from SCIAMACHY in limb and nadir geometries.

Nitrogen dioxide (NO_2) plays an important role in the stratospheric ozone chemistry by controlling the ozone abundances through catalytic destruction or by mitigating ozone depletion through reservoir formation. Tropospheric concentrations determine the ozone amount.

Here we present the validation results for the operational version 6.01 nadir NO_2 total column product. The data processor version 6 (as v5.02) is based, for the trace gas slant column retrieval, on the SDOAS algorithm which was created by BIRA-IASB. The retrieval of NO_2 total column data takes into account cloud parameters from the OCRA/SACURA models (Lichtenberg and Hrechanyy, 2015; ESA, 2017). The NO_2 vertical columns are compared with the corresponding old version 5.02 SCIAMACHY product and with the operational GOME-2A NO_2 version 4.6 data product. NO_2 slant columns are furthermore compared with the SCIAMACHY/IUP product which also is based on the new level 1 version 8 radiances and irradiances.

2 Method of comparisons

The total NO_2 has a pronounced daily variation. Thus, we calculated conversion factors for the specific local times and latitudes to make measurements from different satellites and also intra-satellite data comparable.

We used the tabulated photochemical box model PRATMO (McLinden et al., 2006), which is driven by climatological ozone and temperatures. The look-up tables are given as a function of latitude, time, altitude, and SZA. We integrated the NO_2 profiles to get an overall total column conversion factor and build a PRATMO factor database as a function of latitude and SZA. Then, for each NO_2 measurement, one conversion factor is calculated.

The effect of intraday NO_2 changes is displayed in Fig. 2A. Total columns can change quite strongly for certain latitudes. This also has to be taken into account for each satellite scan, as modern sensors have across track swaths in the order of 2000 km.

We calculated relative differences for each pixel in the comparisons of the two SCIAMACHY versions. When comparing GOME-2 measurements, we first computed the mean values for each dataset and afterwards the relative differences.

As the cloud parameters (cloud fraction and cloud top height) have changed (see SCILOV report on clouds), the comparison of both ESA versions 5 and 6 is only done for cloud fractions less than 0.1 to minimize the impact of cloud parameter changes within the field of view.

Global annual means of the differences and the corresponding standard deviations were calculated as shown in Fig. 6. Also, zonal monthly means over the lifetime of the instrument help to find periods of unexpected data behaviour, where parameters differ in one of the datasets. Trend analysis were performed using the robust Theil-Sen linear regression (Sen, 1968).

3 Available datasets

3.1 ESA L2V6 and L2V5 NO_2 total columns

The ESA/DLR operational L2V5.02 and V6.01 NO_2 total column amounts are generated using the Differential Optical Absorption Spectroscopy (SDOAS) algorithm in the 426.5–451.5 nm fitting window (visible spectral range). The BIRA-IASB algorithm employs the GOME Data Processor (GDP) 4.0 and the implementation of the GDOAS algorithm (Van Roozendael et al., 2006). Low frequencies are removed by a polynomial of 2nd order. Absorption cross sections are taken from Bogumil et al. (2003) for O_3 and NO_2 at a temperature of 243 K.

The air mass factors (AMF) used to convert the slant columns to the vertical total columns are calculated with an iterative VCD algorithm, using the LIDORT version 2.2 forward model. The reference wavelength for the AMF calculations using LIDORT is 439.0 nm. The solar zenith angle (SZA) limit for the operational product is 89deg. The SGP 6.01/Y is retrieved using the IPF 8.0X Level-1 data. A description of the NO_2 V6 retrieval code can be found in the ATBD and the README file (Lichtenberg and Hrechanyy, 2015; ESA, 2017). Both versions are basically the same, except for the differences in the level 1 input data.

The cloud parameter input for the NO_2 retrieval is taken from the nadir cloud detection algorithms OCRA/SACURA, used for the retrieval of cloud fraction and top height. While the cloud coverage is derived by OCRA (Loyola, 1998) with updated databases in processor version 6.01, the cloud top height and optical thickness are derived by SACURA (Kokhanovsky et al., 2005).

3.2 ESA and IUP NO_2 slant columns from SCIAMACHY L1V8

The ESA NO_2 slant column retrieval is already described in the previous section. A new IUP NO_2 data product was available for comparisons using the SCIAMACHY L1V8 data (Richter and Burrows, 2002; Richter et al., 2005) with radiance spectra from 425.19-–464.96 nm. NO_2 absorption cross sections are taken from Vandaele et al. (1998) for a gas temperature of 220 K. A polynomial of the 5th order is used for filtering. The solar zenith angle cut off for the IUP product is at 85°. Air mass factor calculations with SCIATRAN (Rozanov et al., 2014) can be used for the conversion to total columns.

3.3 EUMETSAT GOME-2A L2V4.6 NO_2 total columns

The GOME-2 instrument has been flying on Metop-A since October 2006. The GDP 4.6 dataset for GOME-2A was used here for the comparisons. The compared data spans the period from 04.01.2007 until the end of the SCIAMACHY measurements. The NO_2 vertical column accuracy is expected to be in the order of 5-15% for unpolluted cases. The IUP GOME-2A retrievals have not been taken into account in this study.

4 Results

The NO_2 total columns of the newest level 2 version 6 are shown in Fig. 1 for 2007 as an annual mean and the standard deviation of the mean. The NO_2 hotspots are clearly visible in the mean, but also in the standard deviations where the annual cycle is high over industrial regions like Northern Europe, Tehran, Johannesburg, and East China.

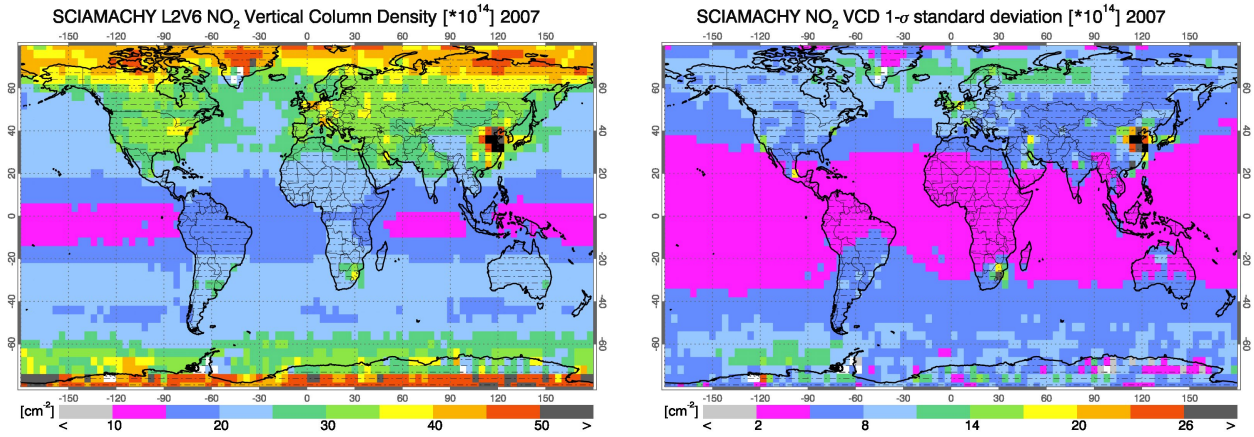

Figure 1: (A) The SCIAMACHY operational level 2 version 6.01 NO_2 product depicted as vertical column density [10^{14} molec cm^{-2}] on a global scale as an annual mean for 2007. The grid boxes are chosen to be $4^\circ \times 4^\circ$ latitude/longitude. The high values towards the poles are due to different local times along the orbit. (B) The corresponding standard deviation of the NO_2 annual mean.

We detected an increase towards the poles which is due to different local times of the measurements along the orbit and has to be taken into account. To compensate the diurnal photochemical effects, a correction factor is applied using the PRATMO model (see Fig. 2 A) that leads to a decrease in the polar NO_2, as shown in Fig. 2(B).

This is also illustrated in the NO_2 zonal monthly mean time series in Fig. 3. Fig. (A) shows the original data and (B) the corrected values, where all NO_2 total columns are set to an arbitrary time of midnight. The time series show a rather smooth inter-annual periodic behaviour. No outliers due to Level 1 data problems are found.

4.1 Relative differences of ESA V5/V6 and IUP NO_2 slant columns

As the ESA V5/V6 retrieval algorithms are basically the same, we do not expect large changes in the slant columns. Nevertheless, the level 1 data product and the cloud parameter product have changed, so that differences can not be ruled out. We first compared the slant columns of ESA level 2 version 5 and 6. The relative differences V5-V6 are plotted for the orbit 40989 in Fig. 4A. Here, all results were taken into account, including the cloudy pixels. A difference of 0.5% with a 1-σ scatter of 1.6% is observed. The V6 slant columns are generally lower. There is also a dependency on latitude/solar zenith angle. The difference is highest for low solar zenith angles and equatorial latitudes. The global annual mean relative difference in 2007 is 0.16 ± 1.86%.

On the other hand, we compared the ESA V6 slant columns with the IUP data product. Although both use the same L1V8 input data, the differences are large, as depicted in Fig. 4B. The IUP slant columns are on average 7.7% lower and the scatter is much higher in comparison to the V5-V6 results. This can be explained by a) different spectral retrieval windows, b) different absorption spectra with c) different temperatures. For instance, a comparison of numerous DOAS codes for ground-based measurements have shown that differences up to 8% are possible (Peters et al., 2017).

A global monthly mean view of the relative differences IUP-ESA NO_2 is shown in Fig. 5 for October 2010. Cloud coverage is not taken into account for this comparison. The lowest differences of

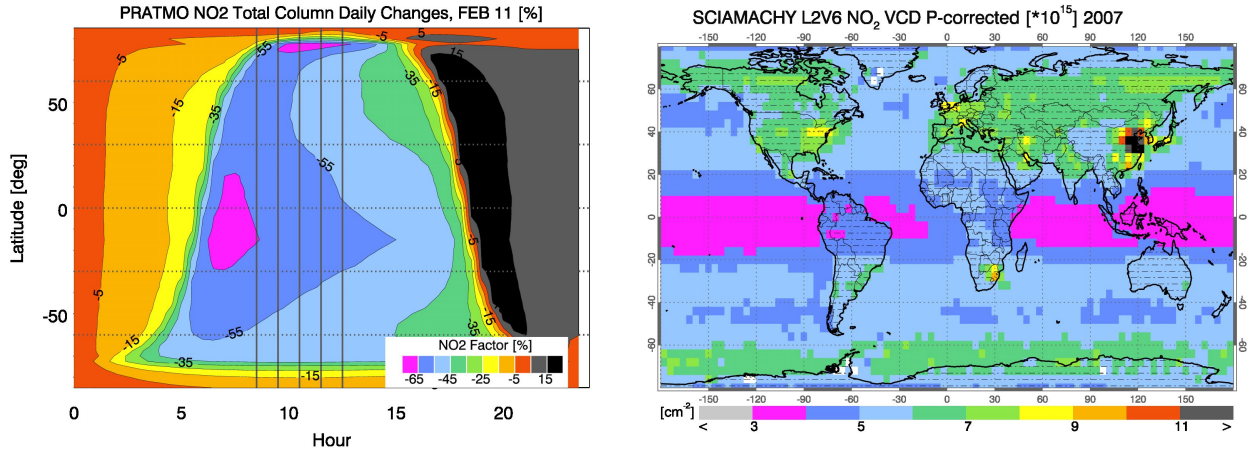

Figure 2: (A) The NO_2 total column daily change [%] from PRATMO conversion factors as a function of day time and latitude for February, 11th. Five possible satellite equator crossing times are superimposed as vertical lines. (B) Global map of annual NO_2 total columns corrected for local time differences. The conversion time is set to 0:00, so that the total columns are roughly twice as large as the uncorrected ones. The high values near the poles are corrected, which were due to large local time differences.

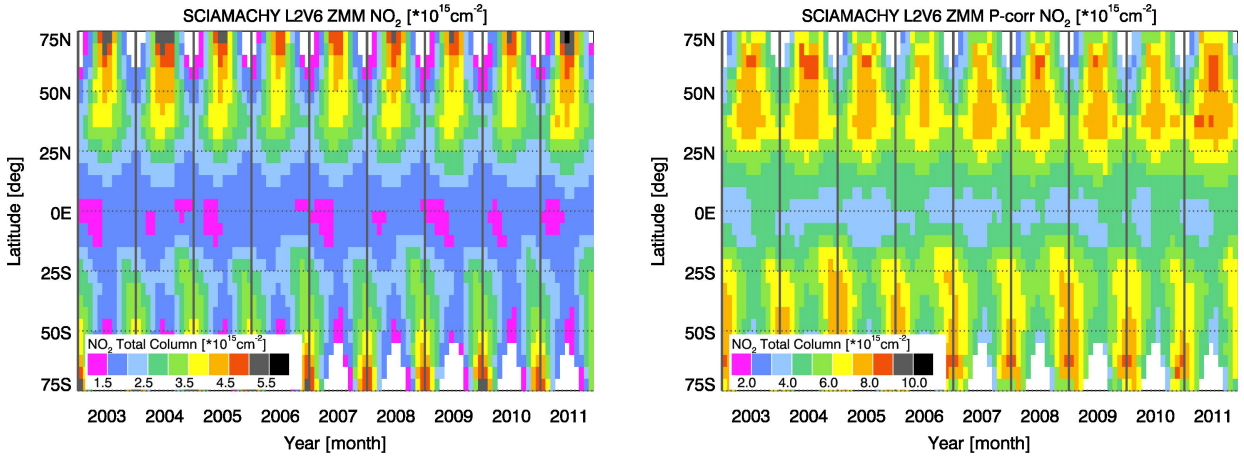

Figure 3: SCIAMACHY NO_2 version 6 zonal monthly means for the period 2003-2011 (A) without correction factors and (B) with correction factors. The latitude bands are 5° wide.

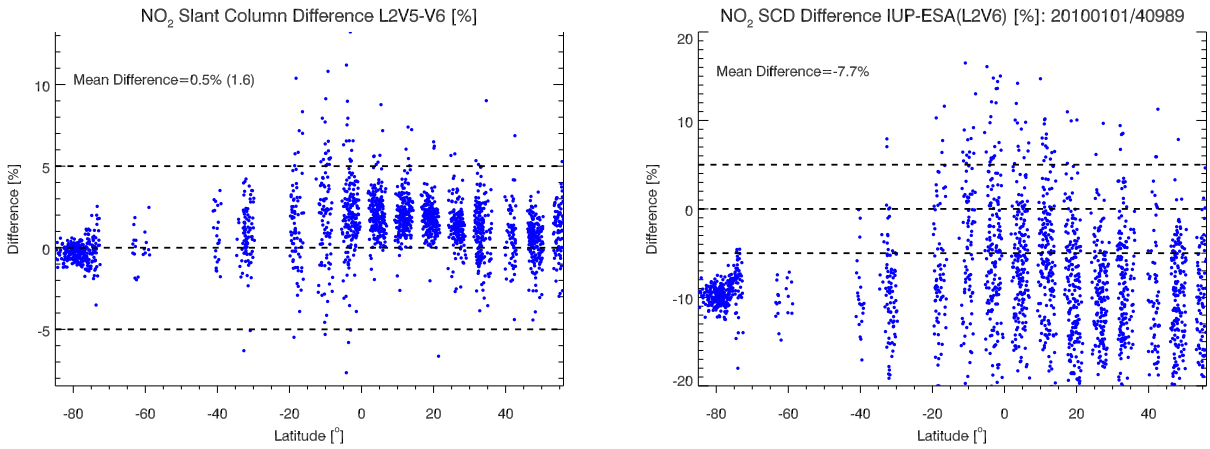

Figure 4: (A) SCIAMACHY NO_2 slant column version 5-6 relative differences for the orbit 40989 on 1 Jan 2010. (B) Relative difference between IUP slant columns and ESA V6 NO_2 for the same orbit.

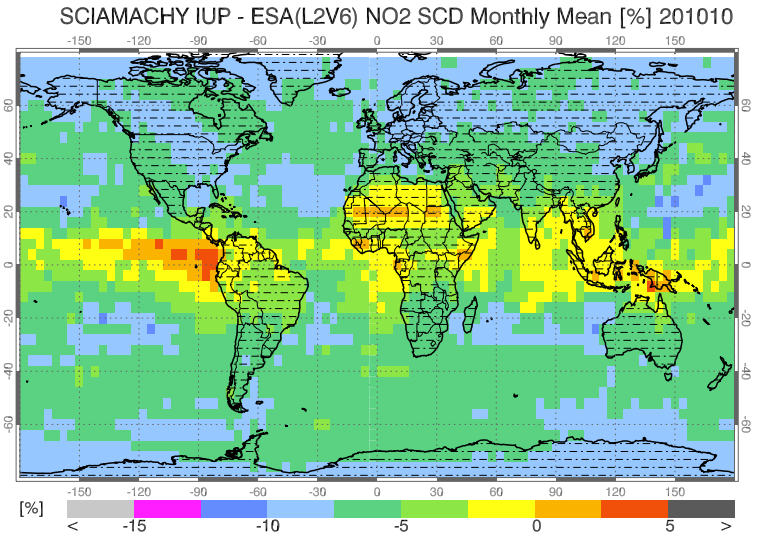

Figure 5: Global map of monthly mean relative differences of IUP-ESA(V6) NO_2 slant columns for October 2010.

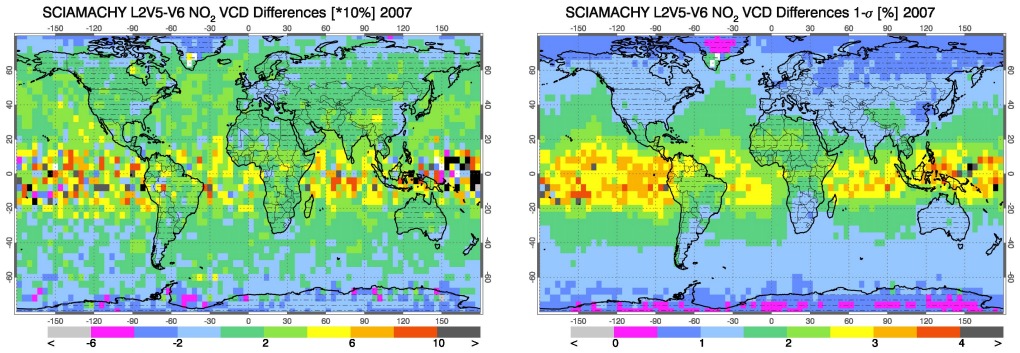

Figure 6: Annual mean of NO_2 total column differences [per mille] between ESA version 5 and 6 and the corresponding standard deviation [%].

$\pm$2.5% occur over bright surfaces (Northern Africa) and in equatorial regions where high clouds are predominant. In all other regions, the IUP NO_2 slant columuns are between -5 and -10% lower.

The ESA/DLR total NO_2 V5.02 has already been compared in SCILOV-10 (Weber et al., 2014) with the IUP NO_2 data product. The agreement was well within $\pm$5% in the tropics and mid latitudes with a insignificant mean bias of 0.8%. The operational NO_2 amounts were higher than the IUP amounts at higher latitudes where differences have reached 15%. This pattern is qualitatively also seen in the comparisons with V6 NO_2 slant columns.

4.2 ESA L2V6 versus L2V5 NO_2 total columns

The overall differences between the two versions 5 and 6 are on average below $\pm$0.2%, as shown in Fig. 6. Taking also the standard deviation into account, the highest differences occur in tropical regions over oceans, where version 6 NO_2 is lower by up to 1%. This is the area of high cloud top heights and low albedo. Although the cloud fraction is limited to 0.1 for these analyses, it seems to be most possible explanation for the larger differences. But cloud fraction and height differences are not unusually large in these areas. So also an Level 1 influence cannot be ruled out.

The temporal evolution of the differences (Fig. 7 A) show a few months of higher deviations that can be linked to the version 5 dataset, which had some high value outliers. These changes must be influenced by the Level 1 radiance changes. Overall the differences are below $\pm$0.4% with a maximum scatter of 2%. The new NO_2 product V6 has in general a much more homogeneous appearance.

A trend analysis using the robust Theil-Sen regression (Sen, 1968) with Spearman correlation coefficients show no significant trends in the differences as shown in Fig. 8. The panel (A) shows the uncorrected version 6 NO_2 total columns for the latitude band [20°N–25°N] and panel (B) the corresponding difference of the versions 5 and 6.

4.3 ESA L2V6 versus GOME-2A L2V4.6 NO_2 total columns

The differences as a function of time (2007-2011) and latitude between the corrected SCIAMACHY NO_2 columns and GOME2A version 4.6 are shown in Fig. 9A. PRATMO atmospheric correction factors for the local time are taken into account, which reduces the differences by roughly 50%. The SCILOV-10 comparisons(Weber et al., 2014) with GOME-2 showed that ESA/DLR V5 NO_2 amounts are higher in the tropics and at high latitudes where differences can reach about 20% for uncorrected data.

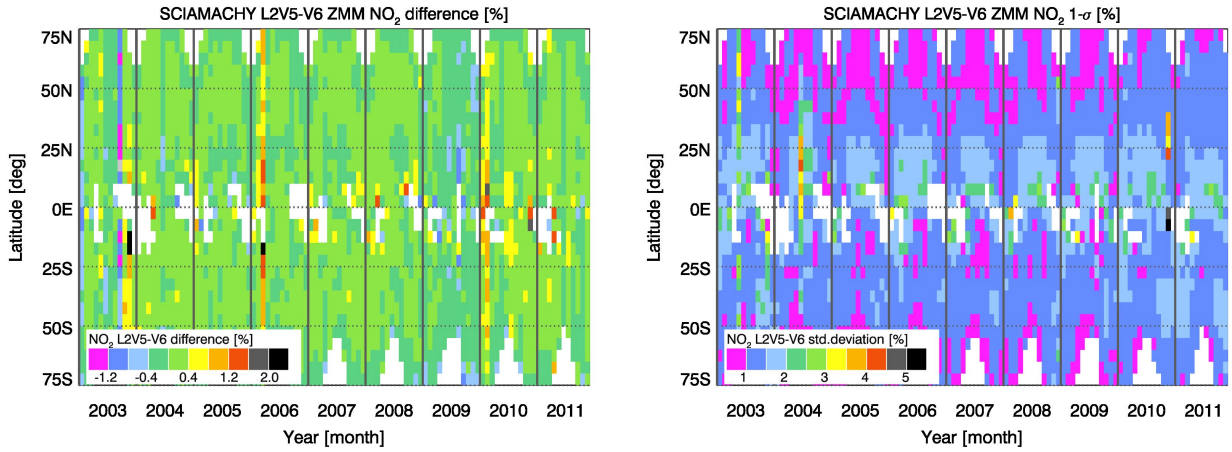

Figure 7: (A) Zonal monthly mean of the NO_2 total column difference of ESA version 5 and 6. (B) Standard deviation of the ZMM total column.

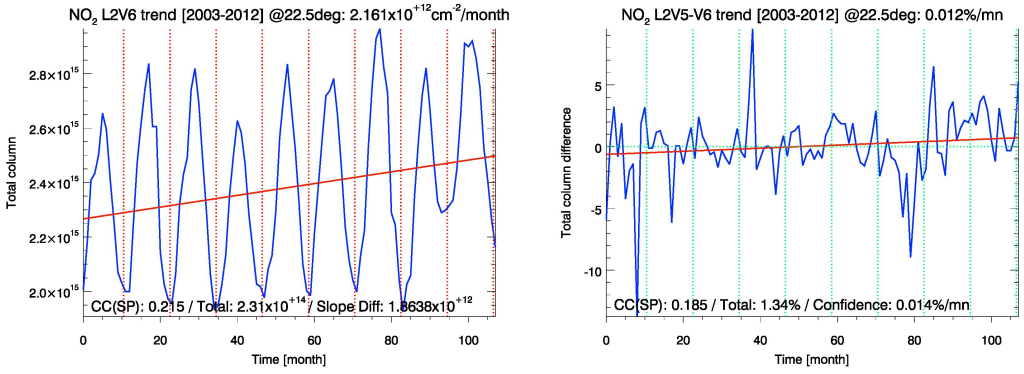

Figure 8: Trend analysis of ESA version 6 NO_2 for the latitude band of 20–25 degree N using the robust Theil-Sen regression. The strong seasonality was not taken into account. (B) Trend of the ESA version 5 and 6 differences. No significant trend is detected. The Spearman correlation coefficient is low and the confidence interval is larger than the calculated trend.

The inter-satellite differences are within roughly $\pm$5%, which is in the range of the accuracy of the methods. The tropics show a positive trend from negative differences of about -20% to positive ones of 10%. There are large intraannual variations in the differences between SCIAMACHY and GOME-2A. No clear trend can be found in the Northern hemisphere, but significant trends were detected in the tropical latitudes and southern hemisphere (B). A total change of 9.2% is observable in the latitude band [-5.0°–0.0°N]. As SCIAMACHY NO_2 showed no trends (see Fig.3), this has to be attributed to the GOME-2A data.

5 Short summary

Even though the NO_2 retrieval method has not changed from version 5 to version 6, the differences between both products are not negligible. Even the slant columns differ by up to 0.5$\pm$1.6% when cloudy pixels are not excluded. Also the scatter of the differences is relatively high.

We calculated conversion factor look up tables, based on PRATMO model data, to deal with pho-

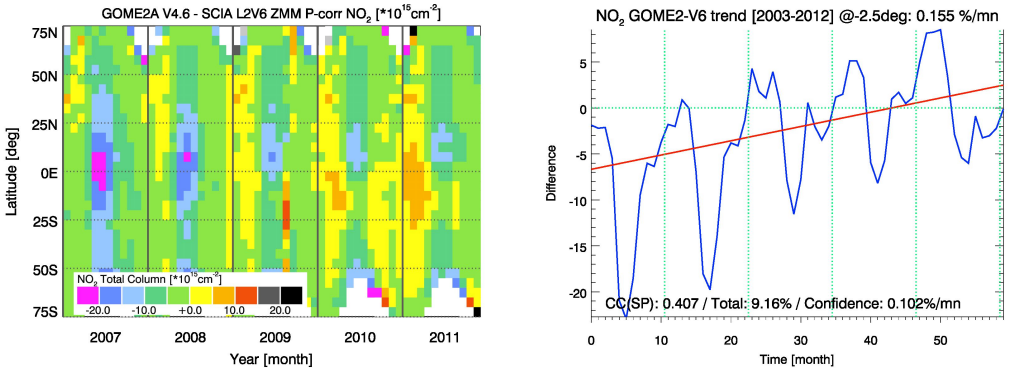

Figure 9: (A) Differences of ZMM time corrected NO_2 total columns [%] between GOME2A version 4.6 and SCIAMACHY version 6. (B) Trend of the differences for the latitude band [-5.0°–0.0°].

tochemical effects due to different sun zenith angles. This is used both for the calculation of global maps and for the comparison between SCIAMACHY and other satellite data.

Comparisons with slant columns from the IUP show larger differences in the order of 7.7% . This is expected, as both products rely on different input parameters (retrieval wavelengths, absorption cross sections).

Due to the new and different cloud product, we restricted the total column comparisons to measurements with cloud fractions less than 0.1. Then, on average, the differences between version 5 and 6 are within $\pm$0.4%. No temporal trends were detected in these differences. The new NO_2 version 6 product is in general a better product, as outliers in the dataset are reduced, when compared to V5.

The comparisons with GOME-2A total columns, using PRATMO correction factors, exhibit differences in the order of 5% globally and over time. But trends exists for some tropical latitude bands that can be attributed to the GOME-2A data.

6 References

Bogumil, K., Orphal, J., Homann, T., Voigt, S., Spietz, P., Fleischmann, O., Vogel, A., Hartmann, M., Bovensmann, H., Frerick, J., , and Burrows, J.: Measurements of molecular absorption spectra with the SCIAMACHY pre-flight model: instrument characterization and reference data for atmospheric remote-sensing in the 230–2380 nm region, Journal of Photochemistry and Photobiology A, pp. 157–167, 2003.

Bovensmann, H., Burrows, J. P., Buchwitz, M., Frerick, J., Noël, S., Rozanov, V. V., Chance, K. V., and Goede, A. P. H.: SCIAMACHY: Mission Objectives and Measurement Modes, J. Atmos. Sci., 56, 127–150, 1999.

Burrows, J. P., Hölzle, E., Goede, A. P. H., Visser, H., and Fricke, W.: SCIAMACHY—Scanning imaging absorption spectrometer for atmospheric chartography, Astron. Astrophys., 35, 445–451, 1995.

ESA: Product Quality README file for SCIAMACHY Level 2 version 6.01 dataset, Technical note ENVI-GSOP-EOGD-QD-16-0132, ESA, 2017.

Kokhanovsky, A. A., Rozanov, V. V., Burrows, J. P., Eichmann, K. U., Lotz, W., and Vountas, M.: The SCIAMACHY cloud products: Algorithms and examples from ENVISAT, Advances in Space Research, 36, 789–799, doi:10.1016/j.asr.2005.03.026, 2005.

Lichtenberg, G. and Hrechanyy, S.: SCIAMACHY Offline Processor Level 1b-2 ATBD Algorithm Theoretical Baseline Document (SGP OL Version 6), Tech. rep., DLR-IMF, 2015.

Loyola, D.: A New Cloud Recognition Algorithm for Optical Sensors, IEEE International Geoscience and Remote Sensing Symposium, 2, 572– 574, 1998.

McLinden, C., Haley, C., and Sioris, C.: Diurnal effects in limb scatter observations, J. Geophys. Res., 111, doi:10.1029/2005JD006628, 2006.

Peters, E., Pinardi, G., Seyler, A., Richter, A., Wittrock, F., Bösch, T., Van Roozendael, M., Hendrick, F., Drosoglou, T., Bais, A. F., Kanaya, Y., Zhao, X., Strong, K., Lampel, J., Volkamer, R., Koenig, T., Ortega, I., Puentedura, O., Navarro-Comas, M., Gómez, L., Yela González, M., Piters, A., Remmers, J., Wang, Y., Wagner, T., Wang, S., Saiz-Lopez, A., García-Nieto, D., Cuevas, C. A., Benavent, N., Querel, R., Johnston, P., Postylyakov, O., Borovski, A., Elokhov, A., Bruchkouski, I., Liu, H., Liu, C., Hong, Q., Rivera, C., Grutter, M., Stremme, W., Khokhar, M. F., Khayyam, J., and Burrows, J. P.: Investigating differences in DOAS retrieval codes using MAD-CAT campaign data, Atmospheric Measurement Techniques, 10, 955–978, doi:10.5194/amt-10-955-2017, 2017.

Richter, A. and Burrows, J. P.: Retrieval of tropospheric NO2 from GOME measurements, Adv. Space Res, 29, 1673–1683, 2002.

Richter, A., Burrows, J., Nuss, H., Granier, C., and Niemeier, U.: Increase in tropospheric nitrogen diox-ide over China observed from space, Nature, 437, 129 – 132, doi:10.1038/nature04092, 2005.

Rozanov, V. V., Rozanov, A. V., Kokhanovsky, A. A., and Burrows, J. P.: Radiative transfer through terrestrial atmosphere and ocean: Software package SCIATRAN, J. Quant. Spectrosc. Radiat. Transfer, 133, 13 – 71, 2014.

Sen, P.: Estimates of the Regression Coefficient Based on Kendall ' s Tau, Journal of the American Statistical Association, 63, 1379–1389, 1968.

Van Roozendael, M., Loyola, D., Spurr, R., Balis, D., Lambert, J.-C., Livschitz, Y., Ruppert, T., Valks, P., Kenter, P., Fayt, C., , and Zehner, C.: Ten years of GOME/ERS-2 total ozone data – The new GOME Data Processor (GDP) Version 4: I Algorithm Description, J. Geophys. Res. – Atmosphere, 111, doi:doi: 10.1029/2005JD006375, 2006.

Vandaele, A. C., Hermans, C., Simon, P. C., Carleer, M., Colin, R., Fally, S., Merienne, M. F., Jenouvrier, A., and Coquart, B.: Measurements of the NO2 absorption cross-section from 42 000 cm-1 to 10 000 cm-1 (238-1000 nm) at 220K and 294 K, J. Quant. Spectrosc. Radiat. Transfer, 59, 171–184, 1998.

Weber, M., Azam, F., Bötel, S., Dikty, S., Lelli, L., Noel, S., Rahpoe, N., Richter, A., Rozanov, A., Schlundt, C., and Weigel, K.: SCILOV10 SCIAMACHY Long-term validation, Tech. rep., IUP, University of Bremen, 2014.